Inverse Problems in Experimental Particle Physics

Sean Gilligan

Abstract

This report presents a survey of the common methods of solving ill-posed inverse problem in experimental high energy physics.

1 Introduction

A common problem faced in the quantitative sciences and their associated technologies is the introduction of errors during the data collection process. While the possible sources of these errors are as varied as the possible events which the data might describe, significant work has been done to develop methods the can help would-be analysts reconcile them. The requisite understanding of a scenario's underlying systematic and stochastic processes might not allow researchers to truly reverse entropy, but it can approximate it with a quantifiable degree of certainty. The applied mathematics that this involves falls within the general category of **inverse problems**, and there are a variety of labels used to refer to the procedures in its arsenal. Within the applications described here there is the colloquially vague **unsmearing**, but there are also names that reference specific applications and methods, such as those characterized in this report.

1.1 The Deconvolution

One way to characterize a basic example would be the following. Assume that data collected regarding n statistical events represent the measurement of n independent and identically distributed (i.i.d.) random variables $\boldsymbol{X} = \{X_1, X_2, \ldots, X_n\}$ from a distribution of possible values represented by the probability density function (PDF) $f_X(x)$, such that the probability of a random variable X_i having a value between x_a and x_b is

$$P(\, x_a < X_i < x_b \,) = \int_{x_a}^{x_b} f(x)\, dx$$

and

$$\int_{\mathcal{X}} f(x)\,dx = 1,$$

where $\mathcal{X}$ represents the domain of x. The error introduced during the measurement process is similarly represented by a set of i.i.d. random variables $\boldsymbol{\varepsilon} = \{\varepsilon_1, \varepsilon_2, \ldots, \varepsilon_n\}$ with a PDF $f_\varepsilon(\varepsilon)$, where the sets $\boldsymbol{\varepsilon}$ and $\boldsymbol{X}$ are typically assumed to be independent of each other. The set of measured values $\boldsymbol{Y} = \{Y_1, Y_2, \ldots, Y_n\}$ then are also i.i.d. and can be defined in terms of the preceding sets of variables such that for event $i \in \{1, \ldots, n\}$,

$$\begin{aligned} Y_i &= g(X_i, \varepsilon_i) \\ &= X_i + \varepsilon_i. \end{aligned} \tag{1}$$

In light of this relationship, the corresponding PDF $f_Y(y)$ can be found explicitly through an operation on $f_X(x)$ and $f_\varepsilon(\varepsilon)$ using the mathematics of functional analysis. Stated in more general terms, the empirical density function f_Y is formed from the **convolution** of the true density function f_X and the error density function f_ε, and is defined by [10]

$$f_Y \equiv f_X * f_\varepsilon \tag{2}$$

$$\begin{aligned} f_Y(y) &\equiv \int_{\mathcal{X}} f_X(x) f_\varepsilon(\varepsilon)\,dx \\ &= \int_{\mathcal{X}} f_X(x) f_\varepsilon\left(g_x^{-1}(y)\right) \left|J_{g_x^{-1}}(y)\right| dx \\ &= \int_{\mathcal{X}} f_X(x) f_\varepsilon(y - x)\,dx, \end{aligned} \tag{3}$$

where J represents the Jacobian of the transformation involved in performing the change of basis on f_ε from ε to x, which is necessary for the evaluation of the integral for a given y. The magnitude of the Jacobian for transformation of ε to $y - x$ through the manipulation of Equation (1) happens to be 1.

As the collection of measured values $\boldsymbol{Y}$ accumulates an estimate of empirical density $\hat{f}_Y$ can readily be formed. However, a major goal in an analysis of data like this is typically to develop an accurate estimate of the true density $\hat{f}_X$. Using the information contained in $\hat{f}_Y$ to accomplish this necessarily requires some attempt at finding an inverse process to the convolution, i.e. the **deconvolution**.

For cases in the form of this particular example there are a variety approaches, but they commonly involve the Fourier transform of the density functions $\{f_X, f_\varepsilon, f_Y\}$ into their corresponding characteristic functions $\{\phi_X, \phi_\varepsilon, \phi_Y\}$ [9][10]. Minor aspects of the definition for the Fourier transform can vary slightly between applications, resulting primarily from the

use of different scale factors and sign conventions. Here it will be defined for some random variable $U \in \mathbb{R}$ with density function $f_U(u)$ and random variable $T \in \mathbb{R}$ as

$$\phi_T(t) = \int_{-\infty}^{\infty} f_U(u)\, e^{itu}\, du. \tag{4}$$

When conditions permit the inverse Fourier transform can be found via

$$f_U(u) = \int_{-\infty}^{\infty} \phi_T(t)\, e^{-itu}\, dt. \tag{5}$$

The Fourier transform is important in deconvolution methods because when you apply it to the convolution of two density functions the link between their respective characteristic functions becomes purely multiplicative, i.e.

$$f_Y = f_X * f_\varepsilon \implies \phi_Y = \phi_X \phi_\varepsilon.$$

An instructional proof of this result is provided on page 447 of [4].

1.2 Generalizing

The remainder of this paper is dedicated to characterizing the major methods adopted by the High Energy Physics (HEP) community toward solving their inverse problems. While most literature on deconvolution methods do use the word "convolution", this operation is also referred to by the German word *faltung* [11]. The latter's English translation, **folding**, is featured prominently in the particle physics community, but refers to a more generalized process than what is described by Equation (3) [8][1][2]. In general, the terms folding and **unfolding** are used to describe two supersets of processes that respectively include convolution and deconvolution.

One way to arrive at the intended generalization is with the help of conditional probability. Thinking of $\{X, Y\}$ as a continuous bivariate random vector with joint PDF $f(x, y)$ and marginal PDFs $f_X(x)$ and $f_Y(y)$, we can define the conditional PDF of Y given that $X = x$ as function of y, $f(y\,|x)$ [6]. The relationship between these PDFs is sufficient to define any one of them in terms of operations involving one or more of the others. As such, for $f_Y(y)$

it can be shown

$$\begin{aligned} f_Y(y) &= \int_{\mathcal{X}} f(x,y)\,dx \\ &= \int_{\mathcal{X}} f(y\,|x) f_X(x)\,dx \\ &= \int_{\mathcal{X}} K(x,y) f_X(x)\,dx. \end{aligned} \tag{6}$$

While integrating over x, $f(y\,|x)$ is implicitly treated a function of both x and y. Acknowledging this allows for understanding Equation (6) as a Fredholm integral of the first kind with a Kernel function $K(x,y)$ reflecting the physical measurement process [3]. The relationship between x and y in $K(x,y)$ is not defined, but when the kernel is a function of the difference of its arguments, such that $K(x,y) = K(y-x)$, Equation (6) becomes the convolution described in Equation (3).

In particle physics experiments, analysts make use of Monte-Carlo (MC) simulations to estimate detector response to randoms samples from some true distribution $f_X(x)^{\text{MC}}$, which is itself estimated by way of MC simulations using models that typically contain theory being tested by the experiment in question. The resulting measured distribution $f_Y(y)^{\text{MC}}$ grants implicit knowledge of $K(x,y)$ by way of Equation (6) [2]. Finding the inverse of this Kernel is then the goal, as it should in theory allow for the mapping of experimental observations $\boldsymbol{Y}$, as randomly sampled from $f_Y(y)$, back to their true values $\boldsymbol{X}$.

1.3 Discretization

In practice researchers are only ever dealing with estimates $\hat{f}_X$, $\hat{f}_Y$, $\hat{f}_X^{\text{MC}}$, and $\hat{f}_Y^{\text{MC}}$, and the sets of data that contribute to these estimates are organized by bin into histograms that form unnormalized granular approximations of the true distributions. Thinking in terms of these histograms allows for the reformulation of Equation (6) into the linear matrix equation:

$$\boldsymbol{\nu} = \boldsymbol{R}\boldsymbol{\mu}. \tag{7}$$

The vectors $\boldsymbol{\nu}$, $\boldsymbol{\mu}$ and matrix $\boldsymbol{K}$ are mapped from their continuous counterparts by [2]:

$$\begin{aligned} \text{true distribution } f_X(x) &\longrightarrow \boldsymbol{\mu} \;\; N\text{-vector of unknowns,} \\ \text{measured distribution } f_Y(y) &\longrightarrow \boldsymbol{\nu} \;\; M\text{-vector of measured data,} \\ \text{Kernel } K(x,y) &\longrightarrow \boldsymbol{R} \;\; \text{rectangular } M\text{-by-}N \textbf{ response matrix}. \end{aligned}$$

The components of vectors $\boldsymbol{\nu}$ and $\boldsymbol{\mu}$ represent the number of events that have occurred within the regions of x and y that define the components' corresponding bins. For $i = 1, \ldots, M$ and $j = 1, \ldots, N$ the components of matrix $\boldsymbol{R}$ are defined by the conditional probability

$$\begin{aligned} R_{ij} &= P(\text{measured value in bin } i | \text{true value in bin } j) \\ &= P(\nu_i | \mu_j), \end{aligned} \tag{8}$$

and so the full response matrix has the form

$$\boldsymbol{R} = \begin{pmatrix} P(\nu_1|\mu_1) & P(\nu_1|\mu_2) & \ldots & P(\nu_1|\mu_N) \\ P(\nu_2|\mu_1) & P(\nu_2|\mu_2) & \cdots & P(\nu_2|\mu_N) \\ \vdots & \vdots & \ddots & \vdots \\ P(\nu_M|\mu_1) & P(\nu_M|\mu_2) & \ldots & P(\nu_M|\mu_N) \end{pmatrix}. \tag{9}$$

With these definitions Equation (7) tells us that an event produced in bin μ_j has some probability ≥ 0 of being measured in each of the M bins of $\boldsymbol{\nu}$, and that each bin count ν_i receives potential contributions from each of the N bins in $\boldsymbol{\mu}$, i.e.

$$\nu_i = \sum_{j=1}^{N} R_{ij} \mu_j. \tag{10}$$

The number of bins are typically set such that $N \leq M$, with the convention $M = N+1$ being common. A higher number of bins in the measured distribution reflects that the measuring process is expected to map some events in $\boldsymbol{X}$ to values of $\boldsymbol{Y}$ that are outside the region of values that define the initial N bins. These one or more extra bins are intended to account for all the possible values that a particular event could be mapped to, such that for a given event starting in bin j one might expect the probabilities of it being measured in each of the M final bins to sum to 1.

However, in practice there are a variety of constraints on events that can either result in them not being included for analysis or even prevent them from being detected at all. For example, an analyst might cut events observed in regions of a detector that result in insufficient data collection, or maybe some event information carriers miss the detector entirely, resulting in such events going unseen. In either case the effect of these missing events is described using the detector **efficiency**, and represented mathematically by the M-vector $\boldsymbol{\epsilon}$, where

component ϵ_j is the efficiency of the jth true bin defined[1] by [7]:

$$\sum_{i=1}^{M} P(\nu_i|\mu_j) = \sum_{i=1}^{M} R_{ij} = \epsilon_j \leq 1. \tag{11}$$

In contrast to this are contributions to measured counts from **background** processes, which are typically studied separately and not involved directly in the unfolding process. Ignoring it would be a major omission in any description of HEP data, so it is briefly included here for completion. Mathematically it is included by modifying Equation (10) to read

$$\nu_i = \sum_{j=1}^{N} R_{ij}\mu_j + \beta_i, \tag{12}$$

where β_i is the ith component of the M-vector $\boldsymbol{\beta}$, which represents the binned background counts. This leads to equations like $\nu_i^{\text{sig}} = \nu_i - \beta_i$ in order to specify the expected number of measured counts that are from the signal of interest. Going forward background will be assumed to already have been accounted for, and ν_i will refer to the measured signal counts of bin i.

As all these variables so far have been derived from the exact continuous distributions $f_X(x)$ and $f_Y(y)$, they correspond to the expectation values that researchers are estimating during data collection and analysis. As this is a counting process the components of the observed number of events $\boldsymbol{n}$ are often related to the components of the expected number of observed counts $\boldsymbol{\nu}$ as a collection of Poisson processes. That is to say the observed counts n_i in bin i are treated as i.i.d. random variables with the probability mass function

$$P(n_i|\nu_i) = \frac{\nu_i^{n_i} \exp -\nu_i}{n_i!}. \tag{13}$$

The counts n_i would in theory then form the estimate $\hat{\nu}_i$ of the expected counts ν_i by

$$\begin{aligned} \nu_i &= E[\hat{\nu}_i] = E[n_i] \\ &= \text{Var}[\hat{\nu}_i] = \text{Var}[n_i]. \end{aligned}$$

Consider an example of the form described by Equation (1), i.e. $Y_i = X_i + \varepsilon_i$. Let the error be i.i.d random variables generated by biasing Gaussian process, $\varepsilon_i \sim N\Big(\mu(x), \sigma(x)^2\Big)$ whose

[1] In the continuous case it is typically written as $\epsilon(x)$, and understood to be the conditional probability of an event producing any measured value given it has a true value of x [@Cowan1998].

mean and variance are functions of x defined by

$$\mu(x) = -2\Big(\log(|x|+1)\Big)^{1/3} \text{ and}$$
$$\sigma(x) = 2\exp\Big(-|x|/30\Big).$$

Next, let X_i be a i.i.d. random variable from a composite distribution of the form $X_i = Z_i X_{1,i} + (1 - Z_i)X_{2,i}$, where

$$X_{1,i} \sim \text{Cauchy}(12, 2),$$
$$X_{2,i} \sim \text{Cauchy}(19, 2),$$
$$\text{and } Z_i \sim \text{Bernoulli}(1/3).$$

So far Figure 1 provides a visualization of unnormalized approximations $\hat{f}_X$ and $\hat{f}_Y$ as histograms resulting from $10,000$ simulations from

2 Unfolding methods in particle physics

2.1 Bin-by-bin

$$\begin{aligned}\hat{\mu}_i &= C_i(n_i - \beta_i) \\ &= C_i\mu_i. \end{aligned} \tag{14}$$

Here, for bin i, β_i represents counted events contributed from background processes and C_i is the **correction factor**. The correction factors are determined by taking the respective ratios of MC simulated truth signal event counts $\left\{\mu_i^{\text{MC}}\right\}$ to the MC simulated reconstructed signal event counts $\left\{\nu_i^{\text{MC}}\right\}$.

$$C_i = \frac{\mu_i^{\text{MC}}}{\nu_i^{\text{MC}}} \tag{15}$$

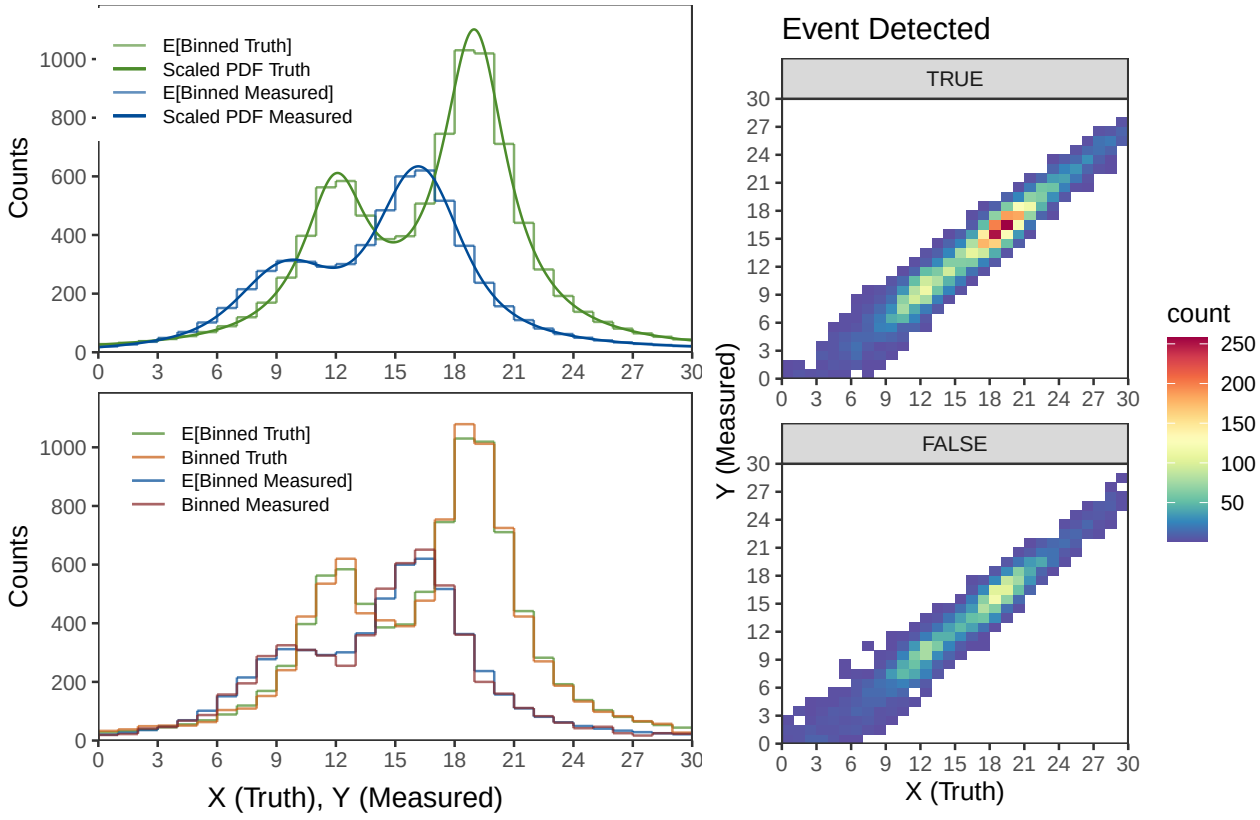

Figure 1: *The above plots feature two bimodal cauchy distributions depicting events before before and after after detector effects. (Top Left) The two continuous distributions correspond to the theoretical PDFs of the two distributions rescaled to correspond with the counts from 10,000 events, and the histograms correspond to the derived expected counts for their respective histograms. (Bottom Left) These four histograms consist of the expected counts as well as possible simulated counts. (Right) These heat maps compare observed and unobserved events as a result of detector efficiency in addition to the detector's smearing effect.*

The expectation value of the estimate $\hat{\mu}_i$ can be calculated to in

$$\begin{aligned} E_i[\hat{\mu}_i] &= C_i E[n_i - \beta_i] \\ &= \frac{\mu_i^{\text{MC}}}{\mu_i^{\text{MC}}} \nu_i \\ &= \left(\frac{\mu_i^{\text{MC}}}{\nu_i^{\text{MC}}} - \frac{\mu_i}{\nu_i^{\text{sig}}} \right) \nu_i^{\text{sig}} + \mu_i \end{aligned} \tag{16}$$

3 Algorithm Construction

Unfolding is ultimately concerned with finding a reliable inverse to the process by which an event occurring in some true bin i maps to an observed bin j. In generalizing this a bit we can think in terms of *causes*, C_i $(i = 1, \ldots, n_C)$ and *effects*, E_j $(j = 1, \ldots, n_E)$, representing the true and observed bins respectively. In regard to a single event we are then interested in conditional probabilistic view for causation, $P(C_i|E_j, I) \equiv \theta_{ij}$, the probability that we can attribute some cause C_i to an observed effect E_j. Using Bayes' theorem we can define this in terms of other probabilities that can be estimated more directly,

$$\begin{aligned} P(C_i|E_j, I) &= \frac{P(E_j|C_i, I) \cdot P(C_i|I)}{\sum_{i=1}^{n_C} P(E_j|C_i, I) \cdot P(C_i|I)} \\ \theta_{ij} &= \frac{\lambda_{ji} \cdot P(C_i|I)}{\sum_{i=1}^{n_C} \lambda_{ji} \cdot P(C_i|I)}, \end{aligned} \tag{17}$$

where the conditional probability regarding inference (effect), $P(E_j|C_i, I) \equiv \lambda_{ji}$, is the probability that some effect E_j will result with some cause C_i and $P_o(C_i|I)$ is the true probability of an event occurring from cause C_i. The term I represents any implicit conditional information regarding the analysis, such as the choice of prior, and is usually apparent when the probabilities are written out as density functions.

At the analysis level we care less about individual events and more about mapping the total number events per effect, $\boldsymbol{x}_E = \{x(E_1), \ldots, x(E_{n_E})\}$, to the total number of events per cause, $\boldsymbol{x}_C = \{x(C_1), \ldots, x(C_{n_C})\}$. However, so far this regards only observed events as categorized into the n_E effects, as we cannot expect to observe or select for all effects resulting from some arbitrary cause C_i. In light of this, while we can add causes to account for any independent background sources to assume the normalization of $P_o(C_i|E_j, I)$ and $P_o(C_i|I)$, such that $\sum_{i=1}^{n_C} P_o(C_i|E_j, I) = 1$ and $\sum_{i=1}^{n_C} P(C_i|I) = 1$, we cannot say the same for $P(E_j|C_i, I)$. A necessarily imperfect effect selection capability results in

$$0 \leq \sum_{j=1}^{n_E} P(E_j|C_i, I) = \sum_{j=1}^{n_E} \lambda_{ji} \equiv \epsilon_i \leq 1,$$

the exact value of which provides for us a definition for ϵ_i, the *efficiency* at which we detect cause C_i from all accounted for observed effects, being also defined and useable as the ratio of observed events resulting from cause C_i to the true number of events resulting from C_i, $x^{obs}(C_i)/x(C_i)$.

A visualization of these lost events can be seen in Figure [2], where some collection of undocumented effects resulting from our collection of causes are lumped into a composite

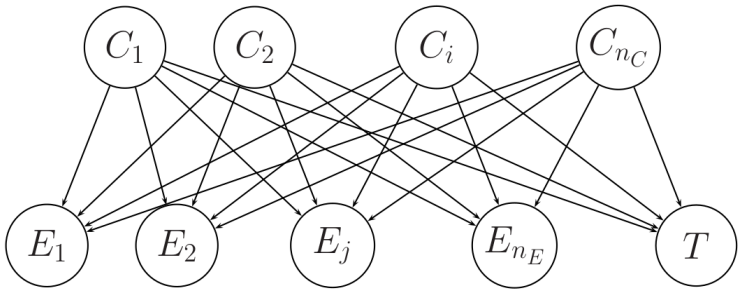

Figure 2: *Thinking of causes and effects as distinct subsets within one or more dimensional cause and effect phase spaces, this figure shows how events are probabilistically mapped from the subsets used to define our causes to the subsets used to define our effects. The node indicated by T ('trash') represents the event selection inefficiency, and can be thought of as an additional effect E_{n_E+1} that contains an unobserved number of events. Unlike the possibility of alloting independent sources of background to different causes, E_{n_E+1} (T) can consist of any number of potentially distinguishable effects depending on how the lost events are distributed across the complement of $\cup(E_1, E_2, \ldots, E_{n_E})$ in our effect phase space.*

effect E_{n_E+1}, which should relate to our efficiency regarding cause C_i by $P(E_{n_E+1}|C_i, I) = \lambda_{n_E+1,i} = 1 - \epsilon_i$. Including this new effect with the others results in $\sum_{j=1}^{n_E} \lambda_{ji} = 1$, creating normalized basis vectors to define the columns of a *smearing matrix* Λ,

$$\begin{aligned} \Lambda &= \begin{pmatrix} P(E_1|C_1,I) & P(E_1|C_2,I) & \ldots & P(E_1|C_{n_C},I) \\ P(E_2|C_1,I) & P(E_2|C_2,I) & \cdots & P(E_2|C_{n_C},I) \\ \vdots & \vdots & \ddots & \vdots \\ P(E_{n_E}|C_1,I) & P(E_{n_E}|C_2,I) & \ldots & P(E_{n_E}|C_{n_C},I) \\ P(E_{n_E+1}|C_1,I) & P(E_{n_E+1}|C_2,I) & \ldots & P(E_{n_E+1}|C_{n_C},I) \end{pmatrix} \\ &= (\boldsymbol{\lambda}_1, \boldsymbol{\lambda}_2, \ldots, \boldsymbol{\lambda}_{n_c}), \end{aligned} \tag{18}$$

where $\boldsymbol{\lambda}_i$ refers to the i-th column consisting of $\{\lambda_{1,i}, \lambda_{2,i}, \ldots, \lambda_{n_E+1,i}\}$.

Now that Eq. (2) accounts for lost events we can begin to construct a conditional probability for $\boldsymbol{x}_C$ similar to that for Eq. (1) using Bayes' theorem,

$$P(\boldsymbol{x}_C|\boldsymbol{x}_E, \Lambda, I) \propto P(\boldsymbol{x}_E|\boldsymbol{x}_C, \Lambda, I) \cdot P(\boldsymbol{x}_C|I), \tag{19}$$

and account for uncertainties in Λ with

$$P(\boldsymbol{x}_C|\boldsymbol{x}_E, I) = \int P(\boldsymbol{x}_C|\boldsymbol{x}_E, \Lambda, I)\ f(\Lambda|I)\ \mathrm{d}\Lambda.$$

At this point one should recognize in Eq. (3) $P(\boldsymbol{x}_E|\boldsymbol{x}_C, \Lambda, I)$ as the likelihood and $P(\boldsymbol{x}_C|I)$ as

the prior in the formal calculation of a posterior. Ignoring the prior for now and focusing on the likelihood, for a given cause C_i we can model this expression as a multinomial distribution such that

$$P(\boldsymbol{x}_E|x(C_i),\Lambda,I) \;=\; \frac{x(C_i)!}{\prod_j^{n_E+1} x(E_j)!}\prod_j^{n_E+1}\lambda_{ji}^{x(E_j)}, \tag{20}$$

which leads us finally to asking how we should estimate our λ_{ji}'s. Once again, using Bayes' theorem we can see that for a fixed i,

$$f(\boldsymbol{\lambda}_i|\boldsymbol{x}_E,x(C_i),I) \;\propto\; P(\boldsymbol{x}_E|x(C_i),\boldsymbol{\lambda}_i,I)\cdot f(\boldsymbol{\lambda}_i|I). \tag{21}$$

Previously mentioned properties about $\boldsymbol{\lambda}_i$ make a Dirichlet($\boldsymbol{\alpha}_{prior_i}$) prior appropriate. A flat prior in which $\boldsymbol{\alpha}_{prior_i} = \{1,\ldots,1\}$ is often chosen, and is done so here. Regardless of the choice for $\boldsymbol{\alpha}_{prior_i}$, multiplying by a multinomial distribution results in the posterior

$$\begin{aligned} f(\boldsymbol{\lambda}_i|\boldsymbol{x}_E,x(C_i),I) \;&\propto\; \left[\frac{x(C_i)!}{\prod_j^{n_E+1} x(E_j)!}\prod_j^{n_E+1}\lambda_{ji}^{x(E_j)}\right]\cdot\left[\frac{1}{\mathrm{B}(\boldsymbol{\alpha}_{prior_i})}\prod_{j=1}^{n_E+1}\lambda_{ji}^{\alpha_{prior_{ji}}-1}\right] \\ &\propto\; \prod_j^{n_E+1}\lambda_{ji}^{\left(\alpha_{prior_{ji}}+x(E_j)\right)-1} \\ &=\; \mathrm{Dirichlet}(\boldsymbol{\alpha}_{prior_i}+\boldsymbol{x}_E). \end{aligned} \tag{22}$$

Samples from this distribution informs much of the the uncertainty resulting from the unfolding process, creating distributions for objects fully or partially calculated from them, such as the smearing matrix, efficiency, and inverse probabilities θ_{ij} once a prior for $P(C_i|I)$ is made. These will be necessary, as $P(\boldsymbol{x}_C|\boldsymbol{x}_E,I)$ becomes the sum of independent multinomial distributions, which does not have a closed solution that we can analytically maximize the likelihood of. We have to make the rest of our progress starting from Eq. (1) where the choice around a prior for $P(C_i|I)$ is due. The choice of $P(C_i|I) = \textit{constant}$ is considered here, which D'Agostini acknowledges is a strong prior that produces biases that will require iterations to be resolved.

Defining $\boldsymbol{\theta}_j = \{\theta_{1,j},\theta_{2,j},\ldots,\theta_{n_C,j}\}$, we can model how the $x(E_j)$ observed events with the effect E_j are likely distributed from potential causes by the multinomial distribution

$$\boldsymbol{x}_C|_{x(E_j)} \;\sim\; \mathrm{Mult}(x(E_j),\boldsymbol{\theta}_j).$$

Before summing over the effects to get the total observed causes we should acknowledge that each $x(E_j)$ is the result of a Poisson process with an unknown rate parameter μ_j. Using the

conjugate prior $\mu_j \sim \text{Gamma}(c_j, r_j)$, with $c_j = 1$ and very small r_j to create a flat prior, we arrive at

$$\mu_j|_{x(E_j)} \sim \text{Gamma}(c_j + x(E_j), r_j + 1),$$

which tells us not to use $x(E_j)$, but μ_j. In dealing with fractional values of μ_j D'Agostini suggests:

1. Rounding μ_j to its nearest positive integer m_j,
2. Sampling from $\boldsymbol{x}_C|_{m_j} \sim \text{Mult}(m_j, \boldsymbol{\theta}_j)$,
3. Rescaling by $\boldsymbol{x}_C|_{\mu_j} = \frac{\mu_j}{m_j}\boldsymbol{x}_C|_{m_j}$,
4. Summing over each effect with $\boldsymbol{x}_C|_{\boldsymbol{x}_E} = \sum_{j=1}^{n_E} \boldsymbol{x}_C|_{\mu_j}$,
5. And applying the inefficiency correction with $\boldsymbol{x}_C = \frac{\boldsymbol{x}_C|_{\boldsymbol{x}_E}}{\epsilon_i}$.

The drawing of multiple samples from the posteriors is used to form an ensemble of values of $\boldsymbol{x}_C$ and estimate credible intervals. The performance of second and later iterations is accomplished by using the previous iteration's posteriors as the new iteration's priors.

4 A Basic Example

In the following example 100,000 random samples are drawn from a Cauchy distribution and then subject to some processes that disperse, bias, and reduce event selection efficiency. The results of these simulations are shown in Figure [3]. The migration matrix does a decent job of demonstrating how the true data was smeared. For unaffected data one would see just a diagonal line from the bottom left to the top right. It was with this in mind that instead of choosing the earlier mentioned flat prior for $\boldsymbol{\alpha}_{prior_i}$ I decided to go with

$$\alpha_{ij} = e^{-|x_{truth} - x_{smeared}|},$$

the values of which are represented in Figure [4].

5 Discussion of Results and Conclusion

The results of my unfolding are shown below in Figure [5]. The iterations get off to an okay start, but instead of converging they begin to behave erratically. The tails blowing

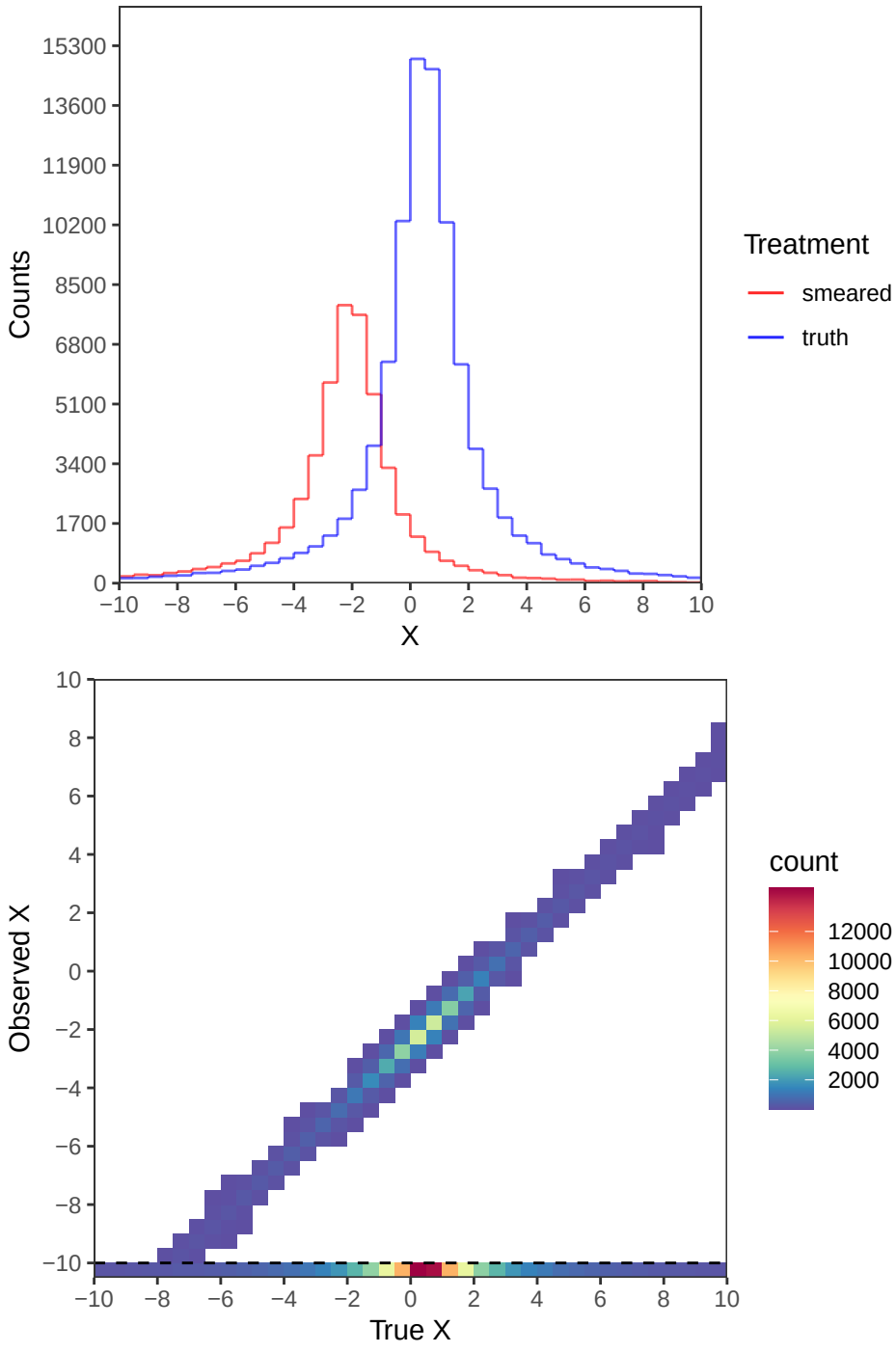

Figure 3: *TOP: The true and smeared distribution of our toy model. BOTTOM: When considering count data, the smearing matrix is often referred to as the response or migration matrix. The bottom row corresponds to the events that were not assigned to an effect.*

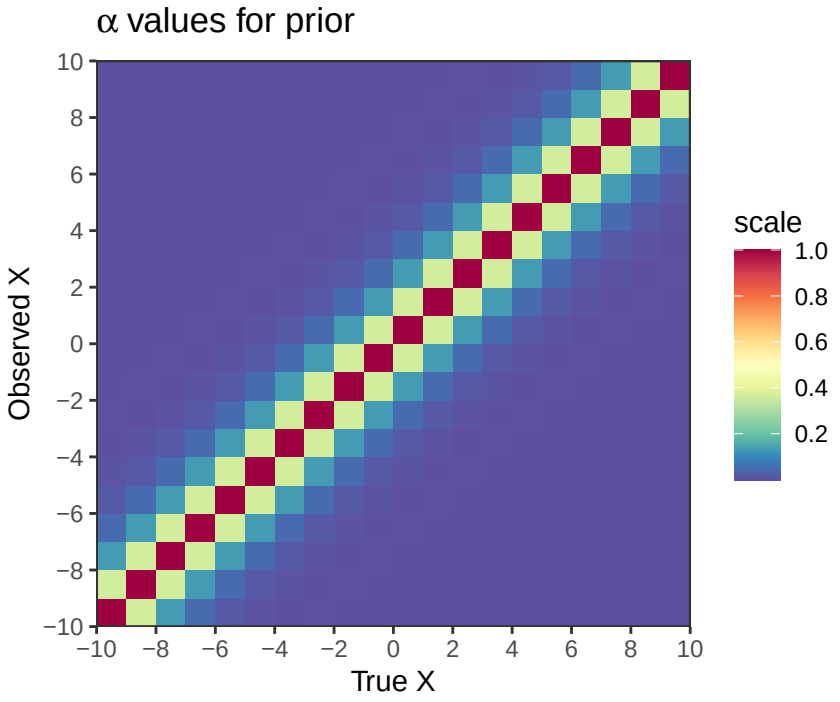

Figure 4: *Instead of choosing a flat prior Dirichlet($\boldsymbol{\alpha}_{prior_i}$) in which $\boldsymbol{\alpha}_{prior_i} = \{1, \ldots, 1\}$, I opted for one that assumed a dominant diagonal signal, corresponding to a max value of alpha along the diagonal that decays exponentially the further you get from the diagonal.*

up clearly comes from using random samples from a posterior distribution as basis for new priors, embedding events in places where there were zero before. I attempted to remedy this with a prior that disfavored events occurring far from the diagonal, as mentioned previously in the context of Figure [4]. It kept these tails from blowing up for at least the first iteration. In the future I will look more into options relating to this issue.

There is almost certainly an error in the code governing the 3rd iteration, resulting in a vastly larger confidence band. Instead of trying to fix this issue I think it would be better use of my time to study some similar working examples [5].

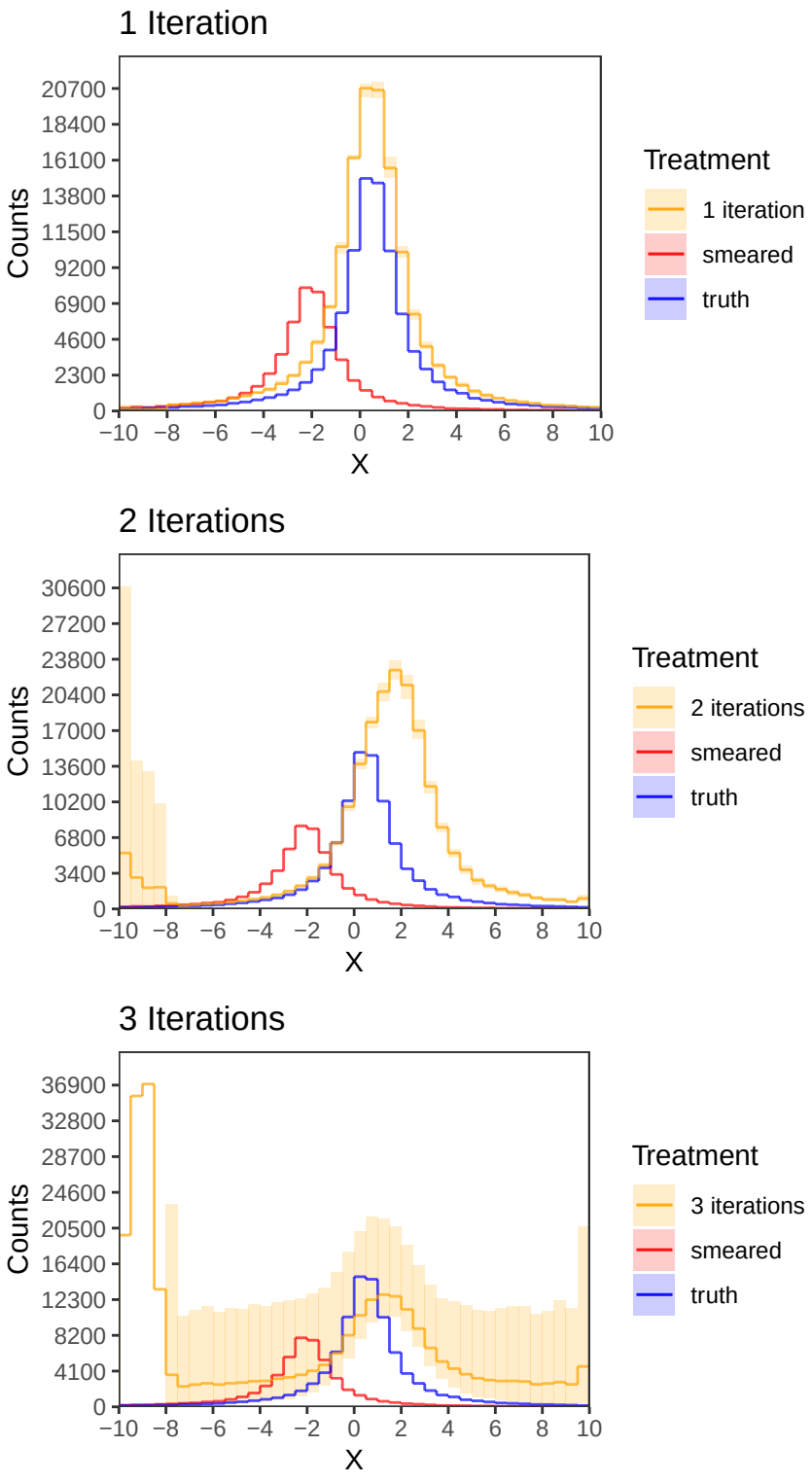

Figure 5: *The first iteration looks like itd heading the right direction. It is my belief that I have an error somewhere in my work.*

A Derivations

A.1 Bin-by-bin

B R Code

The libraries I used are shown here

```
library(tidyverse)
library(gridExtra)
library(knitr)
library(RColorBrewer)
library(gtools)
```

B.1 Code used for Figure [1]

References

[1] Tim Adye. "Unfolding algorithms and tests using RooUnfold". In: *PHYSTAT 2011*. Geneva: CERN, 2011, pp. 313–318. DOI: 10.5170/CERN-2011-006.313. arXiv: 1105.1160 [physics.data-an].

[2] Volker Blobel. "Unfolding". In: *Data analysis in high energy physics: A practical guide to statistical methods*. Ed. by Olaf Behnke et al. Weinheim, Germany: Wiley-VCH, 2013. Chap. 6, pp. 187–226.

[3] Volker Blobel. "Unfolding Methods in Particle Physics". In: *PHYSTAT 2011*. Geneva: CERN, 2011, pp. 240–251. DOI: 10.5170/CERN-2011-006.252. eprint: 1105.1160.

[4] Mary L. Boas. *Mathematical Methods in the Physical Sciences*. Third. Wiley, 2005. ISBN: 9780471198260.

[5] Carsten Daniel Burgard. *RooUnfold*. https://gitlab.cern.ch/RooUnfold/RooUnfold. 2021.

[6] G. Casella and R.L. Berger. *Statistical Inference*. Second. Cengage Learning, 2001. ISBN: 9780534243128.

[7] G. Cowan. *Statistical Data Analysis*. Oxford University Press, USA, 1998. ISBN: 9780198501558.

[8] G. D'Agostini. "A Multidimensional unfolding method based on Bayes' theorem". In: *Nucl. Instrum. Meth. A* 362 (1995), pp. 487–498. DOI: 10.1016/0168-9002(95)00274-X.

[9] Alexander Meister. *Deconvolution Problems in Nonparametric Statistics*. Vol. Lecture Notes in Statistics. Springer, 2009. ISBN: 9783540875567.

[10] Victor M. Panaretos. "A Statistician's View on Deconvolution and Unfolding". In: *PHYSTAT 2011*. Geneva: CERN, 2011, pp. 252–259. DOI: 10.5170/CERN-2011-006.252. eprint: 1105.1160.

[11] Eric W. Weisstein. *Convolution. From MathWorld—A Wolfram Web Resource*. Last visited on 15/2/2022. URL: https://mathworld.wolfram.com/Convolution.html.